



# [<sup>177</sup>Lu]Lu-labeled anti-claudin-18.2 antibody demonstrated radioimmunotherapy potential in gastric cancer mouse xenograft models

Ziqing Zeng<sup>1</sup> · Liqiang Li<sup>1</sup> · Jinping Tao<sup>1</sup> · Jiayue Liu<sup>1</sup> · Hongjun Li<sup>2</sup> · Xueming Qian<sup>2</sup> · Zhi Yang<sup>1</sup> · Hua Zhu<sup>1</sup>

Received: 29 August 2023 / Accepted: 1 December 2023

© The Author(s), under exclusive licence to Springer-Verlag GmbH Germany, part of Springer Nature 2023

## Abstract

**Purpose** Gastric cancer (GC), one of the most prevalent and deadliest tumors worldwide, is often diagnosed at an advanced stage with limited treatment options and poor prognosis. The development of a CLDN18.2-targeted radioimmunotherapy probe is a potential treatment option for GC.

**Methods** The CLDN18.2 antibody TST001 (provided by Transcenta) was conjugated with DOTA and radiolabeled with the radioactive nuclide <sup>177</sup>Lu. The specificity and targeting ability were evaluated by cell uptake, imaging and biodistribution experiments. In BGC823<sup>CLDN18.2</sup>/AGS<sup>CLDN18.2</sup> mouse models, the efficacy of [<sup>177</sup>Lu]Lu-TST001 against CLDN18.2-expressing tumors was demonstrated, and toxicity was evaluated by H&E staining and blood sample testing.

**Results** [<sup>177</sup>Lu]Lu-TST001 was labeled with an 99.17%±0.32 radiochemical purity, an 18.50±1.27 MBq/nmol specific activity and a stability of ≥94% after 7 days. It exhibited specific and high tumor uptake in CLDN18.2-positive xenografts of GC mouse models. Survival studies in BGC823<sup>CLDN18.2</sup> and AGS<sup>CLDN18.2</sup> tumor-bearing mouse models indicated that a low dose of 5.55 MBq and a high dose of 11.10 MBq [<sup>177</sup>Lu]Lu-TST001 significantly inhibited tumor growth compared to the saline control group, with the 11.1 MBq group showing better therapeutic efficacy. Histological staining with hematoxylin and eosin (H&E) and Ki67 immunohistochemistry of residual tissues confirmed tumor tissue destruction and reduced tumor cell proliferation following treatment. H&E showed that there was no significant short-term toxicity observed in the heart, spleen, stomach or other important organs when treated with a high dose of [<sup>177</sup>Lu]Lu-TST001, and no apparent hematotoxicity or liver toxicity was observed.

**Conclusion** In preclinical studies, [<sup>177</sup>Lu]Lu-TST001 demonstrated significant antitumor efficacy with acceptable toxicity. It exhibits strong potential for clinical translation, providing a new promising treatment option for CLDN18.2-overexpressing tumors, including GC.

**Keywords** CLDN18.2 · Lu-177 · Tumor radioimmunotherapy · Radionuclide therapy · Gastric cancer

Ziqing Zeng and Liqiang Li contributed equally to this work.

✉ Zhi Yang  
pekyz@163.com

✉ Hua Zhu  
zhuhuabch@pku.edu.cn

Ziqing Zeng  
z66zq@126.com

Liqiang Li  
liliqiang@bjmu.edu.cn

Jinping Tao  
taojinping2020@163.com

Jiayue Liu  
liujiayue9759@163.com

Hongjun Li  
Hongjun.li@transcenta.com

Xueming Qian  
xueming.qian@transcenta.com

<sup>1</sup> State Key Laboratory of Holistic Integrative Management of Gastrointestinal Cancers, Key Laboratory of Carcinogenesis and Translational Research (Ministry of Education/Beijing), Department of Nuclear Medicine, NMPA Key Laboratory for Research and Evaluation of Radiopharmaceuticals (National Medical Products Administration), Peking University Cancer Hospital & Institute, Beijing 100142, China

<sup>2</sup> Suzhou Transcenta Therapeutics Co., Ltd, Suzhou, Jiangsu 215127, China

## Introduction

GC is a tumor that exhibits moderate sensitivity to radiation [1]. Radiation therapy is widely used in cancer treatment to induce DNA damage in actively proliferating malignant cells. Additionally, radiation exposure can increase antigen exposure, enhance antigen presentation, and assist in reshaping the immune microenvironment and improving the efficacy of immunotherapy [2, 3]. However, the poor tolerance of surrounding organs to external radiation therapy complicates the delivery of radiation [4]. Moreover, compared to localized GC, advanced metastatic GC often cannot be cured by chemotherapy or external radiation alone. In such cases, targeted radioimmunotherapy (RIT) provides an opportunity to deliver radiation selectively to disease sites in patients with metastases, regardless of disease stage, offering a potential clinical treatment strategy for advanced tumor patients. This has been validated by the approval of [ $^{177}\text{Lu}$ ]Lu-PSMA-617 (Novartis, Switzerland) by the FDA for treating prostate cancer [5].  $^{177}\text{Lu}$  is a therapeutic radioactive isotope that emits  $\beta$ -rays, possessing strong tissue penetration and cytotoxicity [6]. When labeling substances such as monoclonal antibodies that specifically target tumor-expressed molecules,  $^{177}\text{Lu}$  can be used to deliver targeted radiation therapy to systemic lesions in patients with tumors such as GC, serving as a powerful tool for preventing and treating systemic micrometastases. Additionally, when properly dosed, this targeted radiation can minimize radiation exposure to healthy tissues, which is an ability not possessed by traditional external radiation therapy [6, 7].

Claudin-18.2 (CLDN18.2) is a member of the human claudin family that plays a crucial role in tight junction structure [8]. It has been reported that over 50% of GC patients express CLDN18.2, with expression rates reaching up to 80% in some populations, and its expression can be observed in both primary and metastatic lesions [9, 10]. Given its highly specific expression in tumors and its greater than 50% expression rate in GC patients, CLDN18.2 a potential target for effective antitumor drug therapy.

In clinical trials, anti-CLDN18.2 antibodies have demonstrated certain antitumor effects in patients with advanced gastric adenocarcinoma [11–13]. Zolbetuximab (IMAB362) is the first antibody targeting CLDN18.2, and when used in combination with first-line chemotherapy, it has promoted longer progression-free survival (PFS) and overall survival (OS) [13, 14].

TST001 is a subsequently developed novel anti-CLDN18.2 monoclonal antibody. Compared to IMAB362, TST001 has higher affinity, stronger Fc $\gamma$ RIIIa binding capacity, increased antibody-dependent cell-mediated cytotoxicity (ADCC) and antibody-dependent cellular phagocytosis (ADCP) activity, and greater antitumor activity due

to reduced fucosylation [15]. In a phase I clinical study (NCT04396821), TST001 in combination with chemotherapy achieved a median PFS of 9.5 months and a median duration of response of 9.9 months in patients with 1st-line advanced gastric and gastroesophageal junction cancer (GC/GEJ).

Recently, clinical trials have demonstrated that targeted RIT can inhibit tumor growth [16, 17] and, in some cases, even eradicate certain types of cancer [18–20]. In terms of safety, RIT agents, including those labeled with  $^{177}\text{Lu}$ , have shown good toxicity control in human patients [21, 22]. From a technical perspective, the TST001 antibody exhibits high tumor uptake and prolonged retention time [23, 24], fulfilling the needed characteristics of a radionuclide therapy probe; additionally, its retention time matches well with the half-life of  $^{177}\text{Lu}$  (6–7 day), making DOTA-TST001 a suitable precursor for RIT probe construction.

In previous studies conducted in our laboratory, we constructed high-resolution positron emission computed tomography (PET) probes that allow comprehensive, real-time, and noninvasive monitoring of CLDN18.2 *in vivo*. The development of therapeutic radionuclide-labeled RIT probes can be synergistic with these diagnostic probes, achieving an integrated approach to the diagnosis and treatment of CLDN18.2-overexpressing tumors, thus providing a more precise and efficient method for combating cancer.

The aim of this study was to construct a CLDN18.2-targeted [ $^{177}\text{Lu}$ ]Lu-labeled RIT probe, namely, [ $^{177}\text{Lu}$ ]Lu-TST001, and evaluate its preclinical antitumor efficacy and safety. In this manuscript, we report significant therapeutic effects and acceptable short-term toxicity of [ $^{177}\text{Lu}$ ]Lu-TST001 in a GC xenograft mouse model, providing a new treatment approach for CLDN18.2-overexpressing tumors, including GC.

## Methods

For detailed information on the supplementary methods, please refer to the Supplementary Materials 2.

### Radiolabeling of [ $^{177}\text{Lu}$ ]Lu-TST001

TST001 was first conjugated with NHS-DOTA (CAS: 170908-81-3), and then DOTA-TST001 was radiolabeled with  $^{177}\text{Lu}$  at pH 5.0 and temperature 37 ° C to achieve radioactive labeling of TST001. The labeling buffer was HCl + NaAc buffer. Please refer to the Supplementary Materials for more details.

## Experiments in xenograft mouse models

To explore the short-term efficacy of the [ $^{177}\text{Lu}$ ]Lu-TST001 probe, the constructed BGC823<sup>CLDN18.2</sup> or AGS<sup>CLDN18.2</sup> subcutaneous xenograft mice were randomly divided into three groups (n=6–8 per group). Each group of mice received a tail vein injection of 50  $\mu\text{L}$  containing 5.55 MBq [ $^{177}\text{Lu}$ ]Lu-TST001, 11.1 MBq [ $^{177}\text{Lu}$ ]Lu-TST001, or 0.9% saline solution. The body weight and tumor size of the mice were monitored before the injection and once a day after the injection. After 15–16 days, the mice were euthanized, and the residual tumor tissue from the treatment group and some normal organs were collected for further studies. In addition, the control experiment of the unlabeled TST001 antibody therapy group was performed using the AGS<sup>CLDN18.2</sup> xenograft mouse model, which was compared with the 0.9% saline control group. These two groups have six mice in each group, and the amount of unlabeled TST001 antibody injected into each mouse remains the same as the amount of antibody injected into the maximum dose probe group (11.1 MBq group, 90  $\mu\text{g}$  TST001 antibody per mouse).

## Toxicity experiment

Mice were monitored daily for toxic reactions such as lethargy, reduced appetite, and skin ecchymosis. In the experiments, tumor-bearing mice were weighed every other day to observe whether there was significant weight loss. In subsequent toxicity experiments, male and female normal BALB/c nude mice (8–10 per sex) were divided into

two groups: one receiving the maximum therapeutic dose (11.1 MBq) and the other receiving saline injection. Blood samples were collected for hematological analysis and liver function testing. Please refer to the Supplementary Materials for more details.

## Statistical analysis

All data were analyzed using a two-tailed t test, and a *p* value less than 0.05 was considered statistically significant. GraphPad Prism 8 was used for data analysis. The results of repeated experiments are presented as the mean  $\pm$  standard deviation unless otherwise stated.

## Results

### Labeling and validation of [ $^{177}\text{Lu}$ ]Lu-TST001

To develop and evaluate a radiolabeled immunotherapeutic probe targeting the CLDN18.2 protein, the unlabeled CLDN18.2-targeted monoclonal antibody TST001 was used, DOTA was used as a bioconjugate and chelating agent, and TST001 was labeled with  $^{177}\text{Lu}$  (Fig. 1A). Through multiple labeling experiments, the specific activity of the labeled product was approximately  $18.50 \pm 1.27$  MBq/nmol, with a radiochemical purity of  $99.17\% \pm 0.32$  (n=4) and a productivity rate of  $51.50\% \pm 3.6$  (n=4), indicating high specific activity and radiochemical purity of the labeled product. The probe product exhibited  $\geq 94\%$

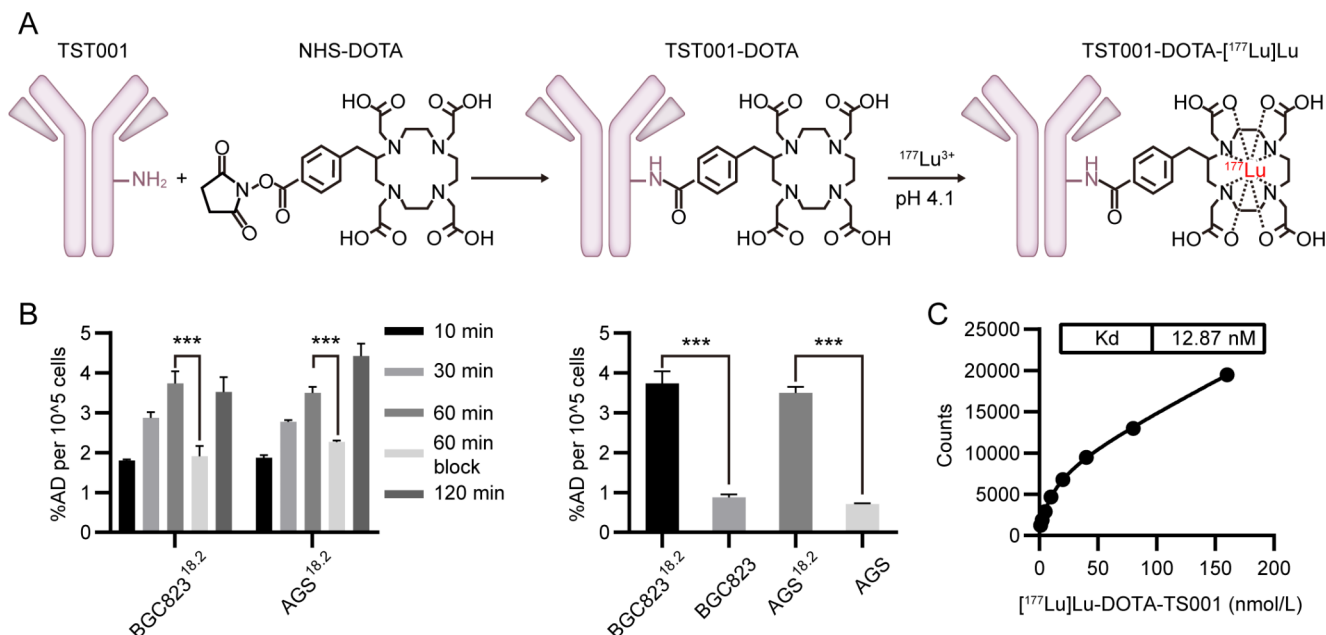


**Fig. 1** Radiolabeling, cell uptake assay and saturation binding experiment. (A) Flow chart of the radiolabeling of [ $^{177}\text{Lu}$ ]Lu-TST001. (B) Cell uptake assay of [ $^{177}\text{Lu}$ ]Lu-TST001 in BGC823<sup>CLDN18.2</sup>/BGC823

and AGS<sup>CLDN18.2</sup>/AGS cells. (C) Cell saturation binding experiment and  $K_d$  calculation of [ $^{177}\text{Lu}$ ]Lu-TST001

stability after incubation at room temperature in PBS and 5% HSA for 7 days (Supplemental Fig. 1).

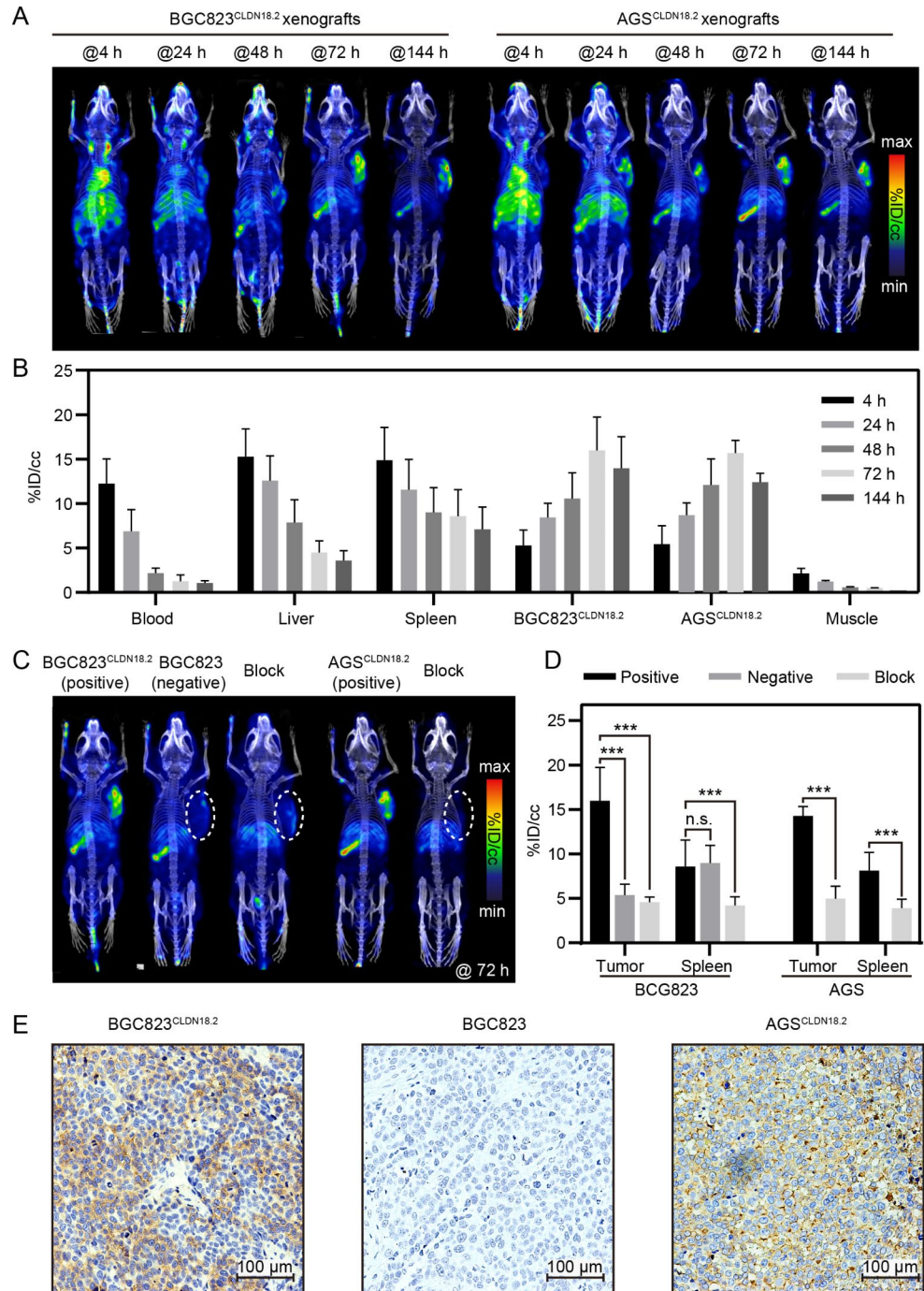
### Specific binding of [<sup>177</sup>Lu]Lu-TST001 to CLDN18.2

CLDN18.2-transfected BGC823 and AGS GC cell lines were used as positive cell lines (BGC823<sup>CLDN18.2</sup>, AGS<sup>CLDN18.2</sup>), and nontransfected BGC823 and AGS GC cell lines were used as negative controls for cell uptake experiments (cell binding assays) to validate the immunoreactivity of the

radiolabeled conjugate to CLDN18.2 protein. The transfected cell lines were confirmed to have higher CLDN18.2 expression than the nontransfected cell lines through flow cytometric analysis (Supplemental Fig. 2). CLDN18.2 expression in xenograft tumors formed by subcutaneous injection of cells in BALB/c nude mice was further confirmed by IHC staining (Fig. 2E, Supplemental Fig. 3).

The cell uptake experiment demonstrated that CLDN18.2-positive cell lines exhibited significantly higher uptake of the radiolabeled probe [<sup>177</sup>Lu]Lu-TST001 compared to the

**Fig. 2** SPECT imaging, ROI analysis and histological verification. **(A)** Imaging of [<sup>177</sup>Lu]Lu-TST001 probe in BGC823<sup>CLDN18.2</sup>/AGS<sup>CLDN18.2</sup> xenograft mouse models. **(B)** ROI analysis of the SPECT imaging of BGC823<sup>CLDN18.2</sup>/AGS<sup>CLDN18.2</sup> models. **(C)** Imaging compares of xenograft between BGC823<sup>CLDN18.2</sup> mouse model and its negative/block group, and the compare between AGS<sup>CLDN18.2</sup> mouse model and its block group. **(D)** Radioactive uptake compares of tumor or spleen between positive/negative/block groups in BGC823 and AGS xenograft models. **(E)** CLDN18.2 IHC staining



negative cell lines, and this uptake could be blocked by excess unlabeled TST001 (at 60 min) (Fig. 1B). The difference between BGC823<sup>CLDN18.2</sup> and BGC823 cells was approximately 4.26-fold, and that between AGS<sup>CLDN18.2</sup> and AGS cells reached 4.94-fold, indicating the specific binding of the probe to the target protein.

Furthermore, using a gradient density plate of BGC823<sup>CLDN18.2</sup> cells, the binding constant (K<sub>d</sub>=12.87 nM) was obtained (Fig. 1C), reflecting a strong binding capability between the probe and the cellular CLDN18.2 protein.

### **[<sup>177</sup>Lu]Lu-TST001 exhibits favorable imaging efficacy and biodistribution in GC mouse models**

In vivo models were constructed using the same cell lines in BALB/c nude mice. Histological staining of tumor tissues derived from BGC823<sup>CLDN18.2</sup> and AGS<sup>CLDN18.2</sup> cell lines showed extensive and homogeneous expression of CLDN18.2, while tumors formed by nontransfected BGC823 cells exhibited low CLDN18.2 expression (Fig. 2E, Supplemental Fig. 3). In BGC823<sup>CLDN18.2</sup>, BGC823, AGS<sup>CLDN18.2</sup>, and AGS subcutaneous xenograft models, small-animal SPECT live imaging experiments were performed using the [<sup>177</sup>Lu]Lu-TST001 probe (n=3). Ex vivo biodistribution experiments were conducted in BGC823<sup>CLDN18.2</sup> and BGC823 models to assess the in vivo CLDN18.2 levels (n=4).

After intravenous injection of approximately 7.4 MBq (200 μCi, 60 μg) [<sup>177</sup>Lu]Lu-TST001, SPECT imaging of the mice was performed. The imaging indicated high tumor uptake in the positive models and low tumor uptake in the negative models (Fig. 2A, C), while other nontarget organs showed relatively low uptake, except for slightly higher uptake in the spleen. IHC confirmed that CLDN18.2 was not expressed in the spleen (Supplemental Fig. 4). In the BGC823<sup>CLDN18.2</sup> model, tumor uptake reached its highest point at 72 h (15.98%ID/cc), and in the AGS<sup>CLDN18.2</sup> model, it also peaked at 72 h (14.29%ID/cc, Fig. 2B). In the block group coinjected with excess unlabeled TST001, the uptake of the two CLDN18.2-positive tumors could be blocked, confirming the specificity of tumor uptake of the probe (Fig. 2C, D).

The ex vivo biodistribution experiments validated the results of the imaging experiments. In BGC823<sup>CLDN18.2</sup> tumor-bearing mice with CLDN18.2 positivity, the [<sup>177</sup>Lu]Lu-TST001 probe exhibited high tumor uptake, which increased over time, reaching its peak (16.57%ID/g) at 48 h postinjection (Fig. 3A). The uptake in other organs decreased with time, and the radioactivity concentration was highest in the blood and spleen, reaching a maximum of 25.55 and 26.03%ID/g, respectively (Fig. 3A). The tumor/

nontumor (T/NT) ratio was also calculated (Supplemental Fig. 5), which represents the ratio of radioactive probe accumulation in the tumor versus nontumor organs. As shown in Supplemental Fig. 5, the T/NT values of all organs increased significantly with time (T/muscle and T/bone first increased and then decreased), indicating that the difference in the distribution of the [<sup>177</sup>Lu]Lu-TST001 probe between tumors and other nonspecific organs became increasingly obvious with time. The tumor uptake in BGC823 tumor-bearing mice without CLDN18.2 expression and in the block-positive model (coinjected with excess unlabeled TST001) decreased to 6.12 and 5.48%ID/g at 48 h, respectively, which was significantly lower than that in the non-blocked CLDN18.2-positive tumors (Fig. 3B), indicating that the probe's high tumor uptake was specific. The biodistribution pattern of the probe in organs in the negative and block groups of mice was similar to that in the positive mice, except for reduced spleen uptake in the block group mice (Fig. 3B).

Based on the biodistribution results in mice, dosimetry calculations for human organ radiation were performed, as shown in Table 1. The highest dose was in the heart wall (2.680 mSv/MBq), followed by the spleen (0.583 mSv/MBq) and the liver (0.534 mSv/MBq). Assuming 35 MBq of [<sup>177</sup>Lu]Lu-TST001 was injected into a human body, the effective radiation dose was less than 4.9 mSv, which is acceptable in routine clinical nuclear medicine practice.

The results from pharmacokinetic experiments in normal KM mice showed that [<sup>177</sup>Lu]Lu-TST001 exhibited favorable pharmacokinetics with a relatively long half-life. The value of the slow half-life was 22.39 h, and the value of the fast half-life was 0.4512 h (Supplemental Fig. 6).

### **[<sup>177</sup>Lu]Lu-TST001 demonstrates compelling therapeutic efficacy in GC mouse models**

Based on the biodistribution and radiation dosimetry estimation results, doses of 5.55 MBq (5.55 MBq) and 11.10 MBq (11.1 MBq) were selected for the administration of the RIT probe [<sup>177</sup>Lu]Lu-TST001 in the animal efficacy study. To evaluate the therapeutic potential of this probe, the BGC823<sup>CLDN18.2</sup> mouse models carrying CLDN18.2-positive xenografts were divided into three groups (n=6), which were treated with 5.55 MBq or 11.1 MBq [<sup>177</sup>Lu]Lu-TST001 and an equal volume of saline solution as a control (100 μL via tail vein injection). In the 5.55 MBq/11.1 MBq treatment groups and the control group, tumor volume and mouse body weight were continuously monitored for 16–17 days. Tumor volume curves were plotted, and significant tumor growth inhibition was observed in the treatment groups compared to the control group (Fig. 4A, \*\*\*: *p*<0.001). For the two treatment doses, the 11.1 MBq group appeared

**Fig. 3** Biodistribution experiments. **(A)** Biodistribution of [<sup>177</sup>Lu]Lu-TST001 in a BGC823<sup>CLDN18.2</sup> mouse model over time. **(B)** Comparison of the biodistribution between positive, negative and block groups of BGC823<sup>CLDN18.2</sup> model at 48 h after injection

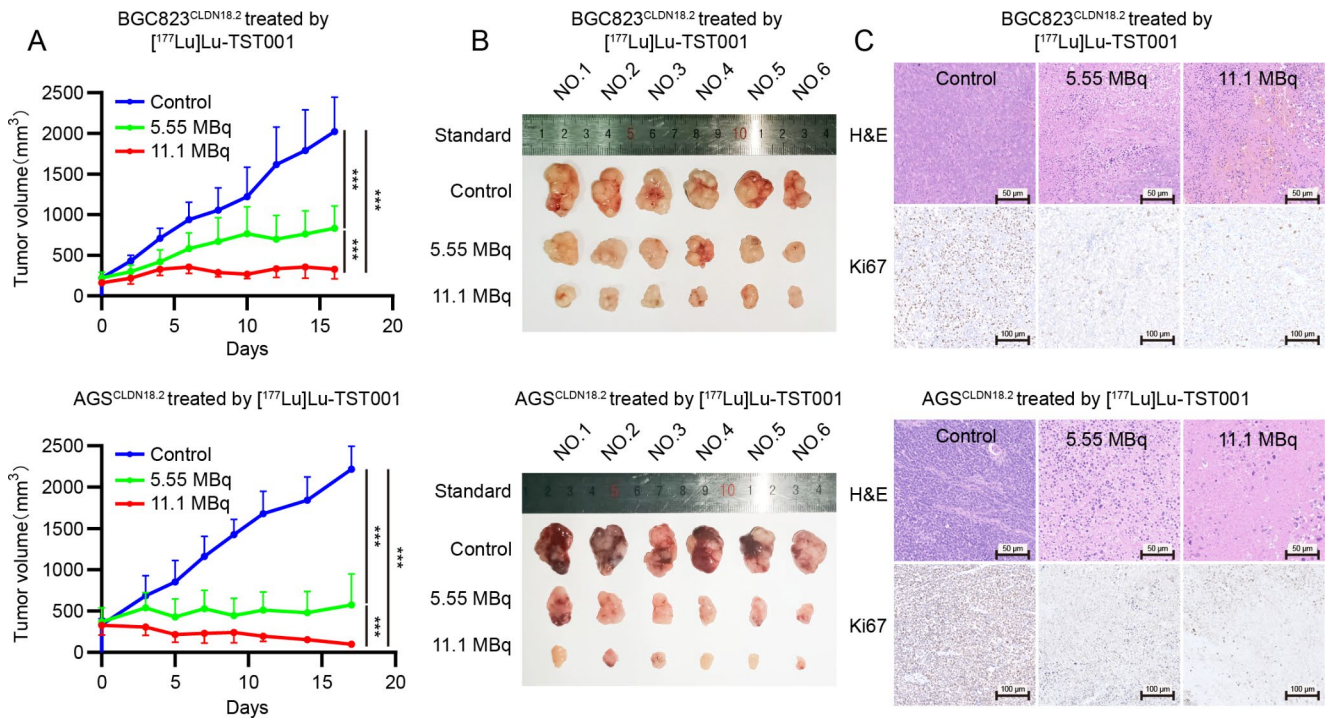
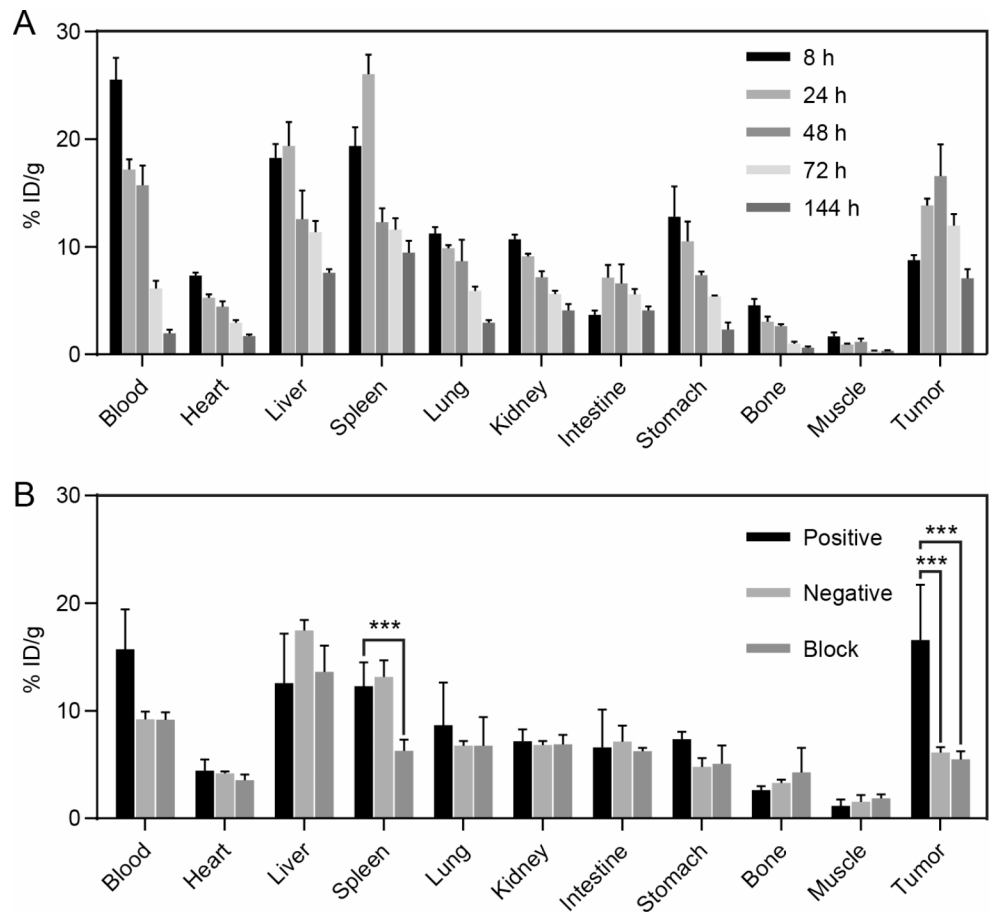


**Fig. 4** The therapeutic efficacy of [<sup>177</sup>Lu]Lu-TST001 in GC mouse models. **(A)** The treatment curves of [<sup>177</sup>Lu]Lu-TST001 in BGC823<sup>CLDN18.2</sup>/AGS<sup>CLDN18.2</sup> models. **(B)** Tumor volume compare between each treatment group of BGC823<sup>CLDN18.2</sup>/AGS<sup>CLDN18.2</sup>

models. **(C)** Tumor H&E and Ki67 IHC staining compare between each treatment group. (H&E bar = 50 μm; IHC bar = 100 μm; \*\*\*: *p* < 0.001)

**Table 1** Human organ absorbed radiation dosimetry estimation of [<sup>177</sup>Lu]Lu-TST001

Target Organ	Absorbed dose (mSv/MBq)
Adrenals	8.21E-02
Brain	6.88E-02
Breasts	7.36E-02
Gallbladder Wall	8.26E-02
LLI Wall	7.18E-02
Small Intestine	3.18E-01
Stomach Wall	1.48E-01
ULI Wall	7.60E-02
Heart Wall	2.68E+00
Kidneys	2.77E-01
Liver	5.34E-01
Lungs	2.86E-01
Muscle	3.54E-02
Ovaries	7.32E-02
Pancreas	8.34E-02
Red Marrow	5.82E-02
Osteogenic Cells	2.20E-01
Skin	6.63E-02
Spleen	5.83E-01
Testes	6.74E-02
Thymus	9.24E-02
Thyroid	6.98E-02
Urinary Bladder Wall	7.04E-02
Uterus	7.32E-02
Total Body	1.15E-01
Effective Dose (mSv/MBq)	1.40E-01

to have better efficacy than the 5.55 MBq group, suggesting a dose-dependent treatment effect. At the end of the 16–17-day observation period, the mice were euthanized, and the BGC823<sup>CLDN18.2</sup> tumors were resected and measured for volume. The tumor volume in the 5.55 MBq group was significantly smaller than that in the control group, and the tumor volume in the 11.1 MBq group was significantly smaller than that in both the 5.55 MBq group and the control group (Fig. 4B). When using TST001 antibodies of the same amount as the 11.1 MBq probe therapy group for treatment, there was no significant difference in tumor volume between the non-radiolabeled TST001 group and the saline group during the treatment (Supplemental Fig. 7). Taken together, [<sup>177</sup>Lu]Lu-TST001 exhibited impressive short-term therapeutic efficacy in GC mouse models.

Given the impressive therapeutic efficacy achieved by [<sup>177</sup>Lu]Lu-TST001 in the BGC823<sup>CLDN18.2</sup> model, to validate the broad applicability of this RIT probe, a treatment experiment was conducted in another GC cell line model, the AGS<sup>CLDN18.2</sup> subcutaneous xenograft model. Since the imaging experiments yielded similar results in both models, the treatment experiment in the AGS<sup>CLDN18.2</sup> model followed the same grouping scheme as the BGC823<sup>CLDN18.2</sup>

model. The results showed that the tumors in the saline control group of the AGS<sup>CLDN18.2</sup> model also progressed rapidly (Fig. 4A). The treatment groups exhibited similar outcomes to the BGC823<sup>CLDN18.2</sup> model: the 11.1 MBq group appeared to have better efficacy than the 5.55 MBq group, and the tumor volume measurements on the last day of treatment indicated that the average tumor volume in the 5.55 MBq group was significantly smaller than that in the control group, while the average tumor volume in the 11.1 MBq group was significantly smaller than that in both the 5.55 MBq group and the control group (Fig. 4B). Furthermore, the efficacy in the AGS<sup>CLDN18.2</sup> model seemed to be superior to that in the BGC823<sup>CLDN18.2</sup> model, as the AGS<sup>CLDN18.2</sup> treatment group not only exhibited an obviously controlled tumor growth curve but also some individual mice showed tumor volumes approaching a near complete response (CR) level (Fig. 4A, B).

In conclusion, [<sup>177</sup>Lu]Lu-TST001 RIT demonstrates profound and persistent antitumor responses in CLDN18.2-positive GC mouse models, achieving impressive antitumor effects even in the low-dose groups.

### Tumor histopathology confirms histological changes induced by the treatment

On the last day of the therapeutic experiment, after euthanizing the mice, the residual tumor tissue at the implantation site was resected and processed. The tissue samples were paraffin-embedded, sliced, and subjected to H&E staining as well as IHC staining for CLDN18.2 and Ki67. H&E staining results revealed that both the BGC823<sup>CLDN18.2</sup> and AGS<sup>CLDN18.2</sup> models in the saline control group exhibited classic tumor tissue structure, while the tumors in the 5.55 MBq and 11.1 MBq treatment groups showed increasingly severe tissue destruction (Fig. 4C). Additionally, the expression of Ki67 in the saline control, 5.55 MBq, and 11.1 MBq groups displayed a progressively decreasing pattern, proportional to the degree of tissue damage, indicating a reduction in tumor proliferation activity (Fig. 4C, Supplemental Figs. 8, 9). The CLDN18.2 IHC staining results showed that, after 11.1 MBq [<sup>177</sup>Lu]Lu-TST001 probe treatment, both models showed a decrease in CLDN18.2 expression of tumor, indicating a decrease in CLDN18.2 antigen levels in tumor tissue after RIT in our experiment (Supplemental Fig. 10).

### [<sup>177</sup>Lu]Lu-TST001 treatment shows no significant short-term toxicity

To assess the toxicity of the probe, 11.1 MBq [<sup>177</sup>Lu]Lu-TST001 or saline solution was administered via tail vein injection to female or male BALB/c nude mice

( $n=4$  per group per sex). After injection, the mice did not exhibit significant toxic reactions, such as drowsiness, loss of appetite, or skin ecchymosis, in either group. Complete blood count analyses within 13 days after injection and liver function on the 13th day were examined and compared between the two groups. The results showed mild hepatotoxicity but no significant heme toxicity associated with  $[^{177}\text{Lu}]\text{Lu-TST001}$  (Fig. 5) in the short term. Complete blood count analyses conducted every other day indicated no significant differences in white blood cells (WBCs), red blood cells (RBCs), and platelets (PLTs) between the 11.1 MBq  $[^{177}\text{Lu}]\text{Lu-TST001}$  injection group and the

saline control group at different time points, and the values remained within the normal range for both female and male mice (Fig. 5). Liver function tests conducted on the 13th day after probe injection revealed no significant changes in ALT and TBIL compared to the saline control group, with only a mild increase in AST (more pronounced in female mice, Fig. 5). Furthermore, mice in each group were weighed every other day until the last day, and none of the groups showed significant weight loss (Supplemental Fig. 11).

After euthanizing the mice on the last day of treatment, selected organs were resected from both the 11.1 MBq  $[^{177}\text{Lu}]\text{Lu-TST001}$  group and the saline control group for

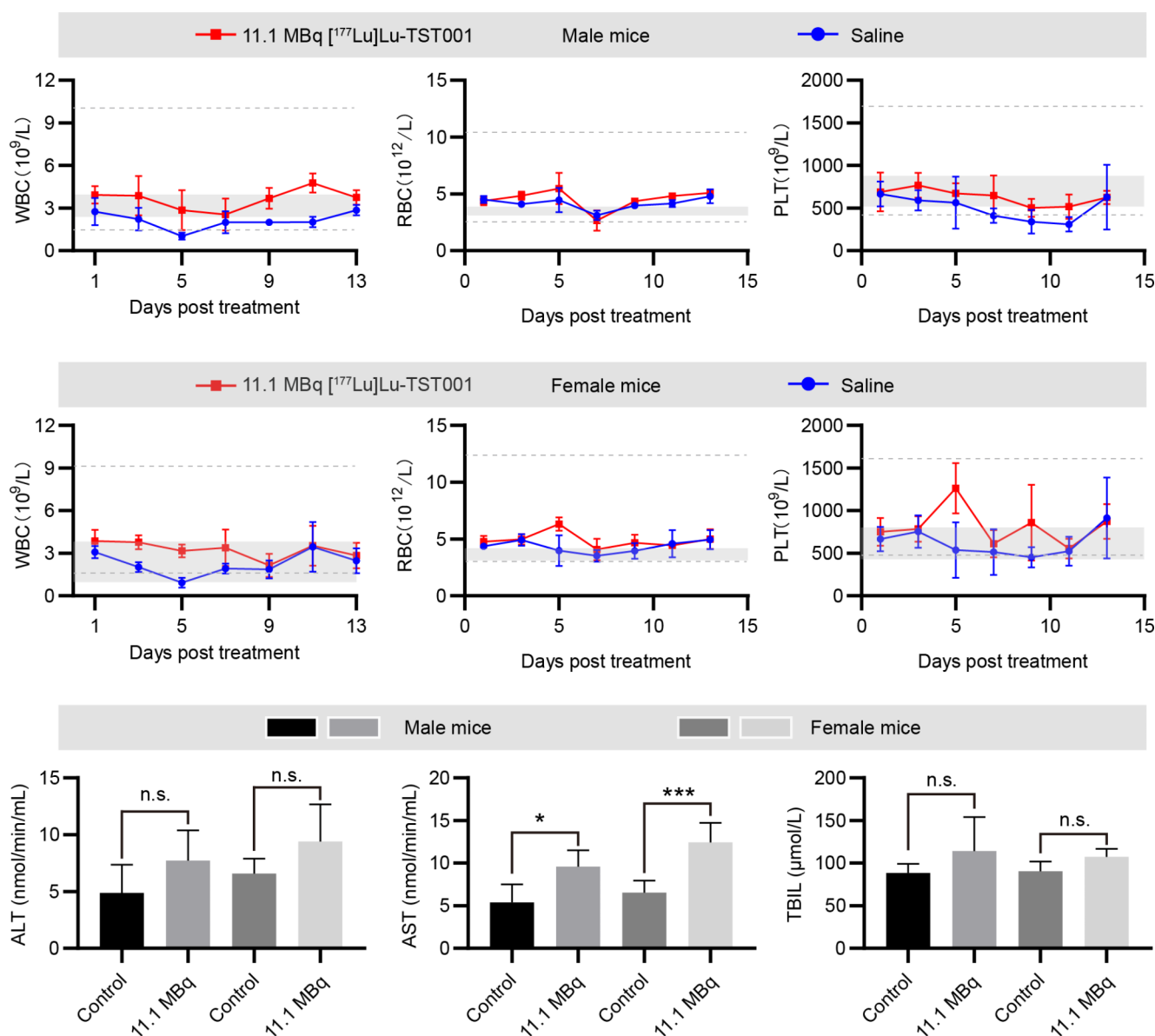


**Fig. 5** Toxicity experiments results. The complete blood count analyses and liver function tests of male or female balb/c nude mice treated with 11.1 MBq  $[^{177}\text{Lu}]\text{Lu-TST001}$  or saline. The grey box represents the mean  $\pm$  SD of the values collected from the entire cohort of toxicity

experiment mouse queue on the day before treatment. The grey dotted line represents the normal range for female or male balb/c mice. (\*:  $p < 0.05$ , \*\*\*:  $p < 0.001$ )

paraffin embedding and sectioning. H&E staining was performed on the sections to observe tissue toxicity. H&E staining results showed no apparent histological damage or other changes in vital organs (including the stomach, liver, spleen, heart, lungs, kidneys, intestines, muscles, etc.) in the probe injection group compared to the saline group (Supplemental Fig. 12). These findings further suggest that the *in vivo* toxicity of [<sup>177</sup>Lu]Lu-TST001 is acceptable.

All the experimental results mentioned above indicate that the therapeutic probe [<sup>177</sup>Lu]Lu-TST001 does not exhibit significant short-term toxicity to vital organs, suggesting its potential application in humans.

## Discussion

The development of new and long-lasting treatments for GC is an urgent clinical need. The emerging target CLDN18.2 has become the most promising therapeutic target in the field of GC. Considering the high specific expression of CLDN18.2 on the membrane surface of GC cells, GMP grade CLDN18.2 antibody TST001 is a promising treatment choice. Currently, TST001 has already entered in Phase III clinical trial (TranStar 301), having a broad application prospect. The emergence of targeted RIT offers the possibility to achieve this goal by combining the specific targeting of CLDN18.2 with the good cytotoxic effects of radiation.

In this study, a [<sup>177</sup>Lu]Lu-TST001 probe was developed that targets CLDN18.2 using a DOTA-TST001 as a precursor and is labeled with <sup>177</sup>Lu, a therapeutic radionuclide. The good molecular imaging, favorable biodistribution, and pharmacokinetics of [<sup>177</sup>Lu]Lu-TST001 were validated in a GC mouse model. The timepoints where peak tumor uptake was reached in SPECT imaging is 72 h, while in biodistribution is 48 h, we think this may be due to slight differences in the total injected protein mass of the two batches of products used for imaging and biological distribution experiments. The injected protein mass of the labeled products used for imaging experiments is relatively high, therefore, the timepoints where peak tumor uptake was reached of imaging experiment were slightly later than the biodistribution experiment. Imaging and biodistribution data indicated potential toxic risks to the heart wall and spleen, but histology confirmed no obvious tissue damage in the hearts and spleens of the model mice, and no significant abnormalities were observed in mouse blood cell counts, suggesting acceptable heart and spleen toxicity. Negative CLDN18.2 IHC confirmed the nonspecific uptake in the spleen, suggesting that the high uptake in the spleen in SPECT and biodistribution may be due to the enhanced ADCC/ADCP effects of TST001 [15]: the combination of Fc receptor on the immune cells and TST001 Fc fragment leads to TST001

retention in the spleen. A similar phenomenon also occurred in a previous study by our laboratory on the construction of the imaging probe Zr<sup>89</sup>-DFO-TST001 [23]. Heart uptake is not high in biological distribution experiments, and the relatively high estimated human dosimetry of the heart wall may be related to the calculation method. In the future, further verification is needed for the dosimetry of this probe in humans. Interestingly, although CLDN18.2 is highly expressed in normal gastric mucosa, CLDN18.2 is buried inside the tight junction of gastric mucosa, normal antibody sized molecules cannot bind to the CLDN18.2 protein of normal gastric tissue through the tight junction supramolecular complex [8, 25]. Therefore, the uptake of this probe by the stomach cannot be seen during imaging and biodistribution experiments.

Moreover, this study explored the short-term therapeutic efficacy of [<sup>177</sup>Lu]Lu-TST001 RIT against CLDN18.2-positive tumors and determined the optimal therapeutic dose in a GC animal model. Safety under the treatment dose of the probe was also examined. Significant therapeutic effects with acceptable short-term toxicity were achieved in the mouse model. Treatment with radioactive [<sup>177</sup>Lu]Lu-TST001 at doses of 5.55 MBq and 11.1 MBq resulted in significant and persistent antitumor activity in the model mice, accompanied by acceptable hepatotoxicity and no other toxic findings. Tumor growth in both the BGC823<sup>CLDN18.2</sup> and AGS<sup>CLDN18.2</sup> GC models was effectively controlled in both treatment groups, with better tumor volume control, greater tumor tissue destruction and cell proliferation reduction in the 11.1 MBq group. Among the two models, [<sup>177</sup>Lu]Lu-TST001 showed better therapeutic efficacy in the AGS<sup>CLDN18.2</sup> model than in the BGC823<sup>CLDN18.2</sup> model. Comparing the IHC staining of CLDN18.2 expression in both tumor tissues, AGS<sup>CLDN18.2</sup> tumor tissue exhibited a higher expression level of CLDN18.2, reaching over 95%, while the expression of CLDN18.2 in BGC823<sup>CLDN18.2</sup> tumor tissue was approximately 70–80%, which is slightly lower. Therefore, the increased targets might be the reason for the better antitumor efficacy of the probe in the AGS<sup>CLDN18.2</sup> model. Additionally, the differential sensitivity of different tumor cells to DNA damage may also contribute to response differences. In addition, non-radiolabeled TST001 group (the same TST001 amount as the 11.1 MBq probe therapy group) didn't show significantly efficacy, which also suggested that the therapeutic effect of the [<sup>177</sup>Lu]Lu-TST001 probe originates from targeted radiation irradiation rather than the monoclonal antibody itself.

According to previous studies, several antibody conjugates labeled with <sup>177</sup>Lu have been tested in clinical trials, and their toxicity in human patients has been well established and controlled [21, 22]. Moreover, increasing evidence suggests that RIT and targeted RIT may inhibit tumor

growth [16, 17] and even eradicate certain types of cancer [18–20]. The TST001 monoclonal antibody targeting CLDN18.2 has also entered clinical trials, demonstrating both safety and efficacy [15, 23]. This study confirmed the compelling therapeutic efficacy, acceptable toxicity in animal models, and acceptable estimations of human radiation dose for [ $^{177}\text{Lu}$ ]Lu-TST001, suggesting the feasibility of clinical applications of this RIT probe. Previous studies in our laboratory have demonstrated good *in vivo* tracking ability of CLDN18.2 in mice and humans using diagnostic PET probes labeled with  $^{89}\text{Zr}$ -TST001 or  $^{124}\text{I}$ -18B10 (TST001 was humanized from 18B10, a mouse-derived hybridoma antibody) [23, 26]. In particular,  $^{124}\text{I}$ -18B10 successfully demonstrated the distribution of CLDN18.2 protein throughout the body in patients with gastrointestinal tumors [26]. In addition, the same-day immunoPET imaging tracers targeting CLDN18.2 are available, such as  $^{68}\text{Ga}/^{18}\text{F}$ -labeled nanobody tracers probing CLDN18.2 [27]. Therefore, these PET probes can serve as diagnostic and whole-body monitoring tools prior to or during treatment with [ $^{177}\text{Lu}$ ]Lu-labeled therapeutic probes, effectively selecting potential beneficiaries of targeted RIT and enabling integrated tumor diagnosis and treatment. Furthermore, noninvasive *in vivo* imaging can also be performed using SPECT instrumentation following injection of [ $^{177}\text{Lu}$ ]Lu-TST001.

In regard to the choice between high and low radiation doses, there are slight differences between mice and humans. However, insights can be gained from mouse experiments. In situations where toxicity is acceptable, we believe it is preferable to prioritize treatment probes with higher radiation doses to achieve better antitumor effects. However, if significant adverse reactions occur, the dose can be reduced as necessary while still maintaining a certain level of tumor control. In future research, the possibility of administering small doses multiple times should be explored, aiming to maintain the antitumor effects of RIT while minimizing systemic toxicity. This approach is supported by previous studies [21, 22] and the observed expression of CLDN18.2 in residual tumor tissue after probe injection.

The toxicity results of this study suggest that the liver may be the main affected organ. However, among the three common liver function indicators, only AST showed an increase. The increase was less pronounced in males. Furthermore, considering the absence of significant abnormalities in the H&E staining of liver tissues from the treatment group as well as the results of biodistribution, the lack of severe liver toxicity in the short term could be concluded.

These preclinical results from our study warrant further clinical evaluation of the therapeutic effects of the [ $^{177}\text{Lu}$ ]Lu-TST001 probe in patients with tumors expressing high levels of CLDN18.2, confirming the promising therapeutic potential of this probe in GC patients with high

expression of CLDN18.2. Additionally, although this study primarily focused on validating the efficacy of targeted RIT against CLDN18.2 in GC, considering the upregulation of CLDN18.2 expression in numerous common tumors, such as pancreatic cancer (> 50%), esophageal cancer, and lung cancer [9], this therapeutic probe holds potential for broader application in all malignancies with high CLDN18.2 expression. In these patients, [ $^{177}\text{Lu}$ ]Lu-TST001 can become a new choice for tumor treatment and can be used as an attempt when traditional treatment methods fail. Meanwhile, due to its targeted tumor killing effect, the probe is particularly suitable for patients with advanced metastasis or those with potential metastatic lesions.

## Conclusion

In conclusion, this study represents the first application of the therapeutic radionuclide [ $^{177}\text{Lu}$ ]Lu-labeled CLDN18.2-targeting antibody TST001. A series of preclinical experiments were conducted to confirm the significant efficacy and low short-term toxicity of the [ $^{177}\text{Lu}$ ]Lu-TST001 probe in preclinical GC tumor models. This probe demonstrates great potential as an RIT drug for clinical application, which may offer a promising new treatment option for CLDN18.2-overexpressing tumors, including GC, leading to improved survival outcomes.

**Supplementary Information** The online version contains supplementary material available at <https://doi.org/10.1007/s00259-023-06561-1>.

**Acknowledgements** The authors sincerely appreciate all the researchers who participated in this study.

**Author contributions** Drs. Ziqing Zeng and Liqiang Li contributed equally to this work.

**Funding** This study was financially supported by the National Natural Science Foundation of China projects (No. 82203612, 82171973, 82171980, 82102092, and 82172604), Capital's Funds for Health Improvement and Research (No. 2022-2Z-2154 and 2022-2Z-2155).

**Data availability** The datasets used and/or analyzed in this study can be obtained from the corresponding authors as reasonably required.

## Declarations

**Competing interests** Intellectual properties protection have been filed by Suzhou Transcenta Therapeutics Co., Ltd., inventor of Xueming Qian; Hongjun Li, and Beijing Cancer Hospital, inventor of Hua Zhu; Yang Zhi. All authors declare that they have no known competing financial interests or personal relationships that could have appeared to influence the work reported in this paper.

**Consent to publish** The manuscript is approved by all authors for publication.

**Ethics approval and informed consent** All animal experiments were approved by the Peking University Cancer Hospital Animal Care and Use Committee (reference number: EAEC 2022-01).

## References

- Wang P, Zhou H, Han G, Ni Q, Dai S, Huang J, et al. Assessment of the value of adjuvant radiotherapy for treatment of gastric adenocarcinoma based on pattern of post-surgical progression. *World J Surg Oncol*. 2021;19:205. <https://doi.org/10.1186/s12957-021-02304-4>.
- Kammerer-Jacquet SF, Deleuze A, Saout J, Mathieu R, Laguerre B, Verhoest G, et al. Targeting the PD-1/PD-L1 pathway in renal cell carcinoma. *Int J Mol Sci*. 2019;20. <https://doi.org/10.3390/ijms20071692>.
- Luo L, Lv M, Zhuang X, Zhang Q, Qiao T. Irradiation increases the immunogenicity of Lung cancer cells and irradiation-based Tumor cell vaccine elicits tumor-specific T cell responses in vivo. *OncoTargets and Therapy*. 2019;12:3805–15. <https://doi.org/10.2147/ott.S197516>.
- Cheng Y, Dong Y, Hou Q, Wu J, Zhang W, Tian H, et al. The protective effects of XH-105 against radiation-induced intestinal injury. *J Cell Mol Med*. 2019;23:2238–47. <https://doi.org/10.1111/jcmm.14159>.
- Fallah J, Agrawal S, Gittleman H, Fiero MH, Subramaniam S, John C, et al. FDA approval Summary: Lutetium Lu 177 Vipivotide Tetraxetan for patients with metastatic castration-resistant Prostate Cancer. *Clin Cancer Res*. 2023;29:1651–7. <https://doi.org/10.1158/1078-0432.Ccr-22-2875>.
- O'Donoghue JA, Bardiès M, Wheldon TE. Relationships between Tumor size and curability for uniformly targeted therapy with beta-emitting radionuclides. *J Nuclear Medicine: Official Publication Soc Nuclear Med*. 1995;36:1902–9.
- Hindié E, Zanotti-Fregonara P, Quinto MA, Morgat C, Champion C. Dose deposits from 90Y, 177Lu, 111In, and 161Tb in Micrometastases of various sizes: implications for Radiopharmaceutical Therapy. *Journal of nuclear medicine: official publication. Soc Nuclear Med*. 2016;57:759–64. <https://doi.org/10.2967/jnumed.115.170423>.
- Türeci O, Koslowski M, Helftenbein G, Castle J, Rohde C, Dhaene K, et al. Claudin-18 gene structure, regulation, and expression is evolutionary conserved in mammals. *Gene*. 2011;481:83–92. <https://doi.org/10.1016/j.gene.2011.04.007>.
- Sahin U, Koslowski M, Dhaene K, Usener D, Brandenburg G, Seitz G, et al. Claudin-18 splice variant 2 is a pan-cancer target suitable for therapeutic antibody development. *Clin Cancer Res*. 2008;14:7624–34. <https://doi.org/10.1158/1078-0432.Ccr-08-1547>.
- Baek JH, Park DJ, Kim GY, Cheon J, Kang BW, Cha HJ, et al. Clinical implications of Claudin18.2 expression in patients with gastric Cancer. *Anticancer Res*. 2019;39:6973–9. <https://doi.org/10.21873/anticancer.13919>.
- Kyuno D, Takasawa A, Takasawa K, Ono Y, Aoyama T, Magara K, et al. Claudin-18.2 as a therapeutic target in cancers: cumulative findings from basic research and clinical trials. *Tissue Barriers*. 2022;10:1967080. <https://doi.org/10.1080/21688370.2021.1967080>.
- Shitara K, Lordick F, Bang YJ, Enzinger P, Ilson D, Shah MA, et al. Zolbetuximab plus mFOLFOX6 in patients with CLDN18.2-positive, HER2-negative, untreated, locally advanced unresectable or metastatic gastric or gastro-oesophageal junction adenocarcinoma (SPOTLIGHT): a multicentre, randomised, double-blind, phase 3 trial. *Lancet (London England)*. 2023;401:1655–68. [https://doi.org/10.1016/s0140-6736\(23\)00620-7](https://doi.org/10.1016/s0140-6736(23)00620-7).
- Sahin U, Türeci Ö, Manikhas G, Lordick F, Rusyn A, Vynnychenko I, et al. FAST: a randomised phase II study of zolbetuximab (IMAB362) plus EOX versus EOX alone for first-line treatment of advanced CLDN18.2-positive gastric and gastro-oesophageal adenocarcinoma. *Ann Oncol*. 2021;32:609–19. <https://doi.org/10.1016/j.annonc.2021.02.005>.
- Lordick F, Al-Batran SE, Ganguli A, Morlock R, Sahin U, Türeci Ö. Patient-reported outcomes from the phase II FAST trial of zolbetuximab plus EOX compared to EOX alone as first-line treatment of patients with metastatic CLDN18.2+ gastroesophageal adenocarcinoma. *Gastric cancer: Official Journal of the International Gastric Cancer Association and the Japanese Gastric Cancer Association*. 2021;24:721–30. <https://doi.org/10.1007/s10120-020-01153-6>.
- Hristodorov D, Fischer R, Linden L. With or without sugar? (A)glycosylation of therapeutic antibodies. *Mol Biotechnol*. 2013;54:1056–68. <https://doi.org/10.1007/s12033-012-9612-x>.
- Wei W, Liu Q, Jiang D, Zhao H, Kuttyreff CJ, Engle JW et al. Tissue factor-targeted ImmunoPET imaging and Radioimmunotherapy of anaplastic thyroid Cancer. *Advanced science (Weinheim, Baden-Württemberg, Germany)*. 2020;7:1903595. <https://doi.org/10.1002/advs.201903595>.
- Larson SM, Carrasquillo JA, Cheung NK, Press OW. Radioimmunotherapy of human tumours. *Nat Rev Cancer*. 2015;15:347–60. <https://doi.org/10.1038/nrc3925>.
- Green DJ, O'Steen S, Lin Y, Comstock ML, Kenoyer AL, Hamlin DK, et al. CD38-bispecific antibody pretargeted radioimmunotherapy for Multiple Myeloma and other B-cell malignancies. *Blood*. 2018;131:611–20. <https://doi.org/10.1182/blood-2017-09-807610>.
- Cheal SM, Xu H, Guo HF, Patel M, Punzalan B, Fung EK, et al. Theranostic pretargeted radioimmunotherapy of internalizing solid Tumor antigens in human Tumor xenografts in mice: curative treatment of HER2-positive breast carcinoma. *Theranostics*. 2018;8:5106–25. <https://doi.org/10.7150/thno.26585>.
- Cheal SM, McDevitt MR, Santich BH, Patel M, Yang G, Fung EK, et al. Alpha radioimmunotherapy using (225)Ac-proteus-DOTA for solid tumors - safety at curative doses. *Theranostics*. 2020;10:11359–75. <https://doi.org/10.7150/thno.48810>.
- Hennrich U, Eder M. [(177)Lu]Lu-PSMA-617 (Pluvicto(TM)): the first FDA-Approved Radiotherapeutic for treatment of Prostate Cancer. *Pharmaceuticals (Basel Switzerland)*. 2022;15. <https://doi.org/10.3390/ph15101292>.
- Schuchardt C, Zhang J, Kulkarni HR, Chen X, Müller D, Baum RP. Prostate-specific membrane Antigen Radioligand Therapy using (177)Lu-PSMA I&T and (177)Lu-PSMA-617 in patients with metastatic castration-resistant Prostate Cancer: comparison of Safety, Biodistribution, and Dosimetry. *Journal of nuclear medicine: official publication. Soc Nuclear Med*. 2022;63:1199–207. <https://doi.org/10.2967/jnumed.121.262713>.
- Chen Y, Hou X, Li D, Ding J, Liu J, Wang Z, et al. Development of a CLDN18.2-targeting immuno-PET probe for non-invasive imaging in gastrointestinal tumors. *J Pharm Anal*. 2023;13:367–75. <https://doi.org/10.1016/j.jpha.2023.02.011>.
- Teng F, Gu Y, Chai H, Guo H, Li H, Wu X, et al. Abstract 5183: the preclinical characterization of TST001, a novel humanized anti-claudin18.2 mAb with enhanced binding affinity and anti-tumor activity. *Cancer Res*. 2020;80:5183–. <https://doi.org/10.1158/1538-7445.AM2020-5183>.
- Niimi T, Nagashima K, Ward JM, Minoo P, Zimonjic DB, Popescu NC, et al. claudin-18, a novel downstream target gene for the T/EBP/NKX2.1 homeodomain transcription factor, encodes lung- and stomach-specific isoforms through alternative splicing. *Mol Cell Biol*. 2001;21:7380–90. <https://doi.org/10.1128/mcb.21.21.7380-7390.2001>.

26. Wang S, Qi C, Ding J, Li D, Zhang M, Ji C, et al. First-in-human CLDN18.2 functional diagnostic pet imaging of digestive system Neoplasms enables whole-body target mapping and lesion detection. *Eur J Nucl Med Mol Imaging*. 2023. <https://doi.org/10.1007/s00259-023-06234-z>.
27. Wei W, Zhang D, Zhang Y, Li L, Jin Y, An S et al. Development and comparison of  $(^{68}\text{Ga}/^{18}\text{F})/(^{64}\text{Cu})$ -labeled nanobody tracers probing Claudin18.2. *Molecular therapy oncolytics*. 2022;27:305–14. <https://doi.org/10.1016/j.omto.2022.11.003>.

**Publisher's Note** Springer Nature remains neutral with regard to jurisdictional claims in published maps and institutional affiliations.

Springer Nature or its licensor (e.g. a society or other partner) holds exclusive rights to this article under a publishing agreement with the author(s) or other rightsholder(s); author self-archiving of the accepted manuscript version of this article is solely governed by the terms of such publishing agreement and applicable law.